Journal of the Korean Ceramic Society
Vol.26, No.5, PP.645~654, 1989.

Fracture Toughness and Failure Behavior of WC-Co Composites by Fracture Surface Analysis

Dong-Bin Han and J.J.Mecholsky, Jr.
Dept. of Materials Science & Engineering, The Pennsylvania State University
(Received July 25, 1987)

파괴표면분석을 통한 WC-Co 복합재료의 Fracture Toughness 측정방법과 Failure Behavior

한동빈 · J.J Mecholsky, Jr.
Dept. of Materials Science & Engineering, The Pennsylvania State University
(1989년 7월 25일 접수)

ABSTRACT

Specimens of WC-Co were indented to measure the resulting crack size and unindented samples were fractured in 3-point flexure to obtain the strength and to measure characteristic features on the fracture surface. Fracture toughness was determined using fractography and compared to those determined using indentation techniques.

We show that principles of fracture mechanics can be applied WC-Co composites and can be used to analyze the fracture process.

The fracture surfaces were examined by scanning electron microscopy and optical microscopy. Characteristic features observed in glasses, single crystals and polycrystalline materials known as mirror, mist, hackle, and crack branching were identified for these composites. We discuss the importance of fracture surface analysis in determining the failure-initiating sources and the failure behavior of WC-Co composites.

요 약

Indentation 방법에 의한 fracture toughness를 측정하고 crack 형태 [Palmqvist or radial/median]도 관찰하였다. 그리고, 강도는 3-point bending test 방법을 이용하여 측정하였다.

유리, 단결정, 다결정 물질의 파괴표면에 mirror, mist, hackle, crack branching 등의 특징을 만드는 fracture mechanics 원리가 brittle-ductile phases의 WC-Co 복합재료에도 적용되는 여부를, 그리고 이 원리에 의한 fracture toughness 측정방법을 소개하였다.

마지막으로 fracture 원인과 failure 현상을 관찰할 수 있는 파괴표면연구의 중요성을 WC-Co를 예로 논의하였다.

INTRODUCTION

Cobalt bonded WC composites show high fracture toughness, hardness, strength and good wear resistance compared to other carbide or ceramic materials. All of these properties make these composites more attractive for use in challenging environments like those in metal cutting, rock drilling in oil and gas industries and tool inserts. As a consequence, great attention has been given to the evaluation of the mechanical properties of these materials[1-3]. In more recent years, attention has been focused on evaluating the fracture toughness of WC-Co[4-6]. There appears to be, some discussion over the proper test to use in measuring the toughness[7-8]. Single edge notched beam(SENB)[5,8,9], chevron notched beam(CNB)[10], double cantilever beam (DCB)[11-13] and indentation crack tests[14-19] have all been used on these materials to measure the resistance to fracture. These tests do not always provide similar estimates of the valus for fracture toughness.

The most controversy occurs with the small cracks associated with the indentation technique[10-13]. Discussions of whether palmquist type or radial/median type cracks occur and what specific equation should be used has generally been at the focus of the controversies for, not only these materials, but other ceramics as well[7]. However, since most failures in ceramics including WC-Co occur from cracks or defects of the size of indentation cracks[5], their behaviour is important to understand.

INDENTATION TECHNIQUES

Previous failure analyses and toughness measurements were mostly limited to surface microcracking and low indentation loads(<1000 N). Shetty and coworkers[7] reported that fracture in WC-Co cermets obey the Palmqvist crack model because the length of cracks from the ends of the impression made by the indenter is linearly dependent on indentation load rather than the 3/2 power dependence expected for the radial/median crack model. They observed the Palmqvist cracks in cemented carbides by sequential polishing[7] of the indentation impression area while monitoring surface removal. Lankford[8] indicated that the half-penny crack model is observable at higher indentation loads. Thus, there is still some question whether WC-Co fits the Palmqvist crack or half-penny crack models, or both.

The equation for fracture toughness by indentation for WC-Co composites based on the Palmqvist crack model[7,20] is as follows :

$$K_c = 0.089[HW]^{1/2} \quad \cdots\cdots(1)$$

where H is hardness, W, a crack resistance parameter[20,21] which can be obtained from $W=(P-P_0)/4a$, where P is the indentation load and P_0 is an experimentally determined threshold indentation load for cracking, and a is the mean Palmqvist crack length(Fig.1).

Anstis, et al.[18,19] have shown that for many materials, a Vickers indentation can produce a model flaw with which to study the fracture process. The cracks resulting from residual contact stresses during

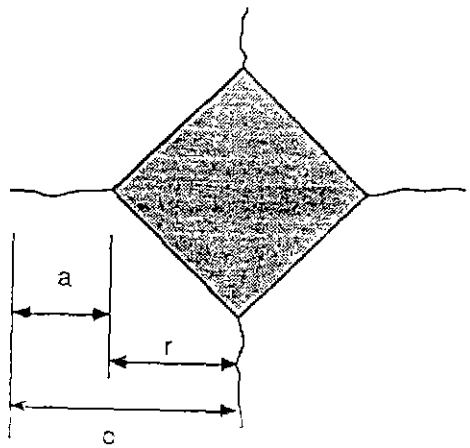

a : Palmqvist crack length
r : half diagonal of impression
c : crack length [a+r]

Fig 1. A schematic illustration of the Vickers indentation and associated parameters.

and after the indentation process can be used to estimate the fracture toughness using a measurement of the crack size from the surface trace(Eq .2) :

$$K_c = 0.016[E/H]^{1/2} Pc^{-3/2} \quad \cdots\cdots(2)$$

where E is the elastic modulus and c is the crack length as shown in Fig.1.

FRACTURE SURFACE ANALYSIS

Fig.2 shows a schematic of the different features observed on the fracture surface of glass, single crystals and polycrystalline materials. These features are known as the failure initiating flaw, the mirror (smooth region), mist(region of small radial ridges surrounding the mirror), hackle(even rougher region of large ridges), and crack branching(two or more primary crack)[22]

Most fracture surfaces can be examined by optical or scanning electron microscopy.

In fine grain materials intergranularly and in larger grain materials failing transgranularly[19], failure sources generally can be easily identified and measured. Without the presence of residual stress,

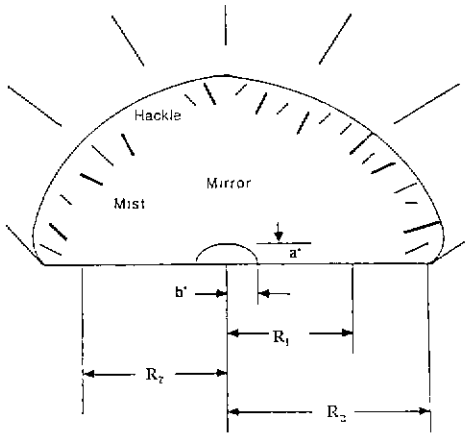

Fig 2. A schematic of the fracture surface including mirror, mist and hackle regions, and macroscopic crack branching.
C* : size of failure-initiating crack ($=\sqrt{a^*b^*}$)
R_1 : mirror-mist boundary
R_2 : hackle-crack branching boundary

fracture toughness can be estimated from fractography[23-25] using equations (3) and (4) :

$$K_c = 1.24\,\sigma_f C^{*1/2} \quad \cdots\cdots(3)$$

C* is the flaw size determined by $C^* = (a^*b^*)^{1/2}$, where a* is the semi-minor axis and b* is the semi-major axis of an elliptical flaw and σ_f is the applied stress at failure ;

$$K_c = 1.24\,M_i[C^*/R_i]^{1/2}, \quad i=1,\ 2,\ 3 \quad \cdots\cdots(4)$$

where M_i is the corresponding mirror constant [MPa $\sqrt{m}$] obtained by $M_i = \sigma_i \sqrt{R_i}$; i=1, 2, 3 corresponds to the mirror-mist, mist-hackle and macroscopic crack branching boundaries, respectively. It should be noted that the measurements of R_i must be made along the tensile surface to use Eq.(4). It has been shown that these mirror constants are generally independent of the rate and type of loading[23,24].

The objective of this study is to introduce another potential method to measure fracture toughness for ceramic-metal composites based upon the principles of the fracture mechanics. This paper also illustrates the importances of fracture surface analysis which provides much information about failure-initiating sources and fracture patterns.

EXPERIMENTAL PROCEDURES

10 wt% and 16 wt% cobalt bonded tungsten carbide composites* were indented with a Vickers diamond. Before indentation, in order to remove the grinding zones on the surface, three sequential steps of polishing were required : 3 minutes with a 15 μm, 10 minutes with a 6 μm, and 10 minutes with a 1 μm diamond compound using an automatic polisher. After polishing, all of the indentations were performed with a Vickers hardness indenter on a compressive testing machine** using loads between 500 N and 2500 N. The loading rates were 0.0008 mm/sec under 1000 N and

* DBS Co. Houston, TX.

** Instron Eng. Corp., Canton, MA.

0.0004 mm/sec for up to 2500 N to avoid indenter damage and any impact effect. The load was held for 15 seconds and released at the same speed as that of the loading. The average crack sizes and hardness impressions were determined by optical microscopy. Also, 14 unindented specimens (as-received*) of these composites were fractured in 3-point bending using Instron machine** for strength measurements and fracture surface analysis. The loading rate for bending test was 0.008 mm/sec.

Fracture surfaces were examined optically, and the features (Fig. 2) were measured with a microscope. Flaw and mirror sizes[μm] were always measured along the tensile surface. In cases where an asymmetric mirror boundary was present, the longer R_1 was used for property evaluation[24].

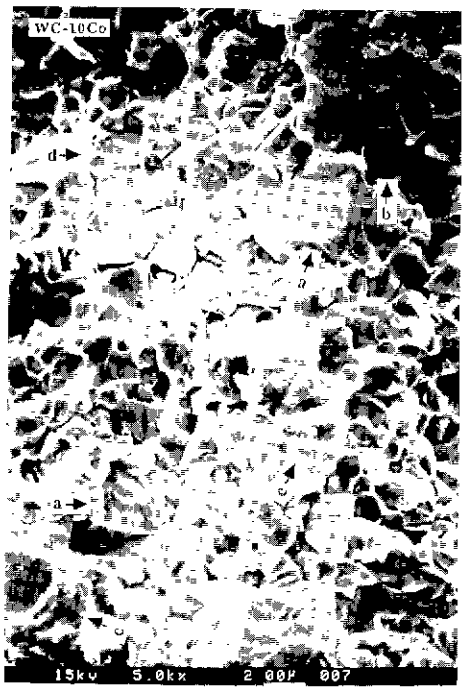

Fig 3. Observation of fracture surface illustrating failure modes in WC-Co composites.
a . fracture of tungsten carbide particle
b : interfacial decoherence of tungsten carbide particle
c : fracture of cobalt phase
d : separation of WC/Co interface

RESULTS AND DISCUSSION

The fracture mode of WC-Co composites is shown in Fig. 3. Measurements of crack size and surrounding topography are presented in Table 1. Table 2 shows the values of strength, hardness, and fracture toughness of 10 wt% Co and 16 wt% Co bonded WC cermets calculated by indentation techniques and fracture surface analysis using the data in Table 1. Fracture toughness values based on $W=(P-P_0)/4a$ (Palmqvist crack model) are relatively high for WC

Table 1. Observed Data from Fracture Surface Analysis of WC-Co Composites.

Sample	a*	2b*	C*	R_1	R_2	R_3	σ_f
			[μm]				[Mpa]
10 Co-a[1]	50	133	58	330	700	1050	1548
10 Co-b	50	70	42	233	500	733	1901
10 Co-c[2]			58	333	500	900	1753
10 Co-d	45	133	55	300	600	1000	1647
10 Co-e[1]	33	100	41	200	400	600	2053
10 C-f[1]	33	100	41	175	430	630	2084
10 Co-g[3]	50	65	40	165	400	600	2273
10 Co-h	45	65	38	200	350	600	2200
10 Co-i[2]			34	230	465	660	1897
10 Co-j	45	65	38	200	400	730	2043
10 Co-k[2]			325	560	1000	1500	772
10 Co-l[1]	45	133	55	250	530	750	1958
10 Co-m[2]			45	250	500	780	1806
10 Co-n[3]	100	150	86	**	**	**	1332
16 Co-a[1]	70	200	118	230	430	660	1626
16 Co-b[2]			46	100	250	400	2190
16 Co-c	45	100	67	150	250	450	2072
16 Co-d[3]	100	150	122	250	600	800	1425
16 Co-e[1]	67	165	105	233	450	700	1638
16 C-f	70	130	95	230	430	700	1607
16 Co-g[2]			75	220	375	550	1776
16 Co-h[3]	45	67	55	100	220	400	2278
16 Co-i	30	75	47	90	200	300	2473
16 Co-j[2]			70	130	300	450	2011
16 Co-k	50	70	59	100	250	400	2277
16 Co-l[1]	40	100	63	135	300	450	2008
16 Co-m[3]	33	65	46	90	170	300	2411
16 Co-n	100	133	115	250	550	800	1480

\+ see Fig. 3 for definition of symbols
1 failure source : elliptical pore
2 failure source : circular pore
3 failure source : machining damage
** no measurement

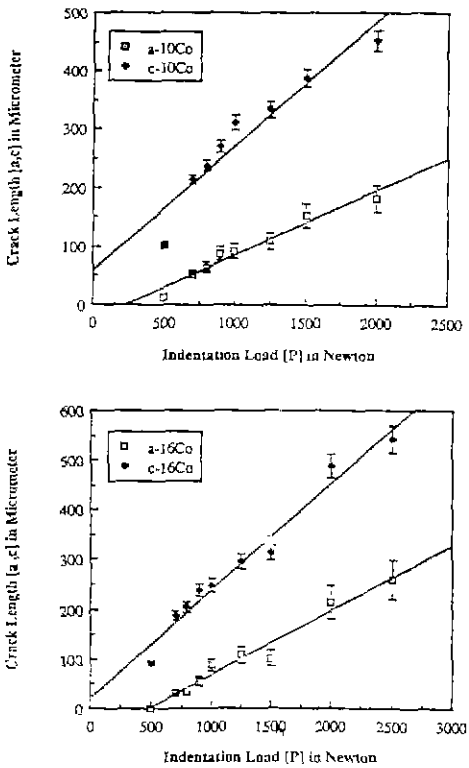

Fig 4. Relation between crack length [a, c] and indentation load[P].

-Co compared to large crack data[6,9-13]. If the classical Palmqvist crack model is used, i.e. with $P_0=0$, then the values would be even higher, and unrealistic. This shows that the Palmqvist crack model is not appropriate for these WC-Co composites regardless of the indentation load. However, if the presumed half-penny crack length(c) is used in place of a in Eq.(1) with $P_0=0$, then reasonable values are obtained for the toughness of WC-Co composite This agreement may be fortuitous or may have significance. Even though there is no justification for using $W=P/4c$, fracture toughness values based on this relationship seem to be acceptable.

Fig.4 shows the average crack sizes (a and c) as a function of indentation loads. The lines exhibit a linear relationship for the Palmqvist crack length (a) and the radial/median crack length (c) vs indentation load (P), rather than the $P^{2/3}$ dependence expected for

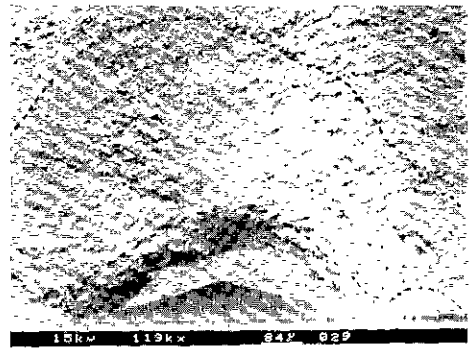

Fig 5. Observation of the fracture surface around an indentation impression exhibiting the crack of radial/median crack shape.

radial/median (half-penny) cracks. In addition, fracture surface analysis in Fig.5 showed that fracture occurred from the median/radial crack shape just below the impression. This implies that the WC-Co fractures from radial/median cracks even if Palmquvist cracks form first. The inconsistent results using indentation techniques strongly suggest that fracture toughness evaluation by the Palmqvist indentation crack model should be reexamined for use with WC

Table 2. Comparisons of Mechanical Properties of WC-Co.

		WC-10 wt%Co	WC-16 wt%Co
Hardness[GPa]		13.8+/-0.6	15.4+/-1.2
Strength[MPa]		1930+/-210	2020+/-350
Fracture Toughness[MPa $\sqrt{m}$]			
Fracture Surface Analysis			
Flaw Size, C*, $\sqrt{ab}$ [Eq.3]		16.2+/-1.2	19.9+/-0.8
Mirror constant [Eq 4]	M_1	15.9+/-1.0	18.7+/-0.7
	M_2	16.4+/-0.7	19.7+/-0.8
	M_3	16 3+/-0 8	19 9+/-0.8
Indentation Techniques		36.5+/-0 8[a]	37.2+/-3.7[a]
		17 7+/-0.7[b]	20 7+/-1.1[b]
		17 5+/-1 3[c]	19.6+/-1.0[c]
Literature Values		13-17[d]	16-21[d]

a. fracture toughness[Eq.1]using Palmqvist crack length (a)

b. fracture toughness[Eq.1]usmg radial/median crack length(c)

c. $K_c=0.016[E/H]^{1/2}Pc^{-3/2}$[Eq 2]

d literature data[large crack model, ref 10, 14, 21]

-Co composites. The toughness values calculated based on the radial/median crack model (Eq.2), however, agree well those obtained using large crack techniques for similar WC-Co composites[4,10].

Fracture toughness by flaw size and mirror constants were summarized in Table 2. For 10 wt% and 16 wt% Co bonded WC, fracture toughness values obtained from fracture surface measurements (Eq.3 and Eq.4) are in good agreement with fracture toughness values calculated from Eq. 2. More data is needed to assure the accuracy of the mirror and crack branching constants, but they are useful as estimates of the toughness for in-service failures of WC-Co components. This study demonstrates that fracture surface analysis developed for glasses and polycrystalline materials can also be applied to WC-Co composites.

SEM photos in Fig.6 show fracture surface features of WC-16 wt% Co composite. The arrows indicate the failure-initiating flaws. In Fig.6-B it is seen that an internal microstructural defect associated with a nonuniformly dispersed Co phase acted as the source of failure. A microprobe unit detected only high cobalt peaks at the failure origin. It has been suggested[26,27] that the formation of cracks around microstructural defects such as agglomerates/aggregates is due to the density difference between the defects and the matrix. The defects have an important role on the density and set up residual stresses which reduce strength[26,27]. Fig.6-B indicates that cracks nucleate at or around weakly linked regions and evidently act as stress concentrators. It is found that stress concentration and residual stress will be higher at the interface and can substantially reduce the load required to fracture materials[28,29].

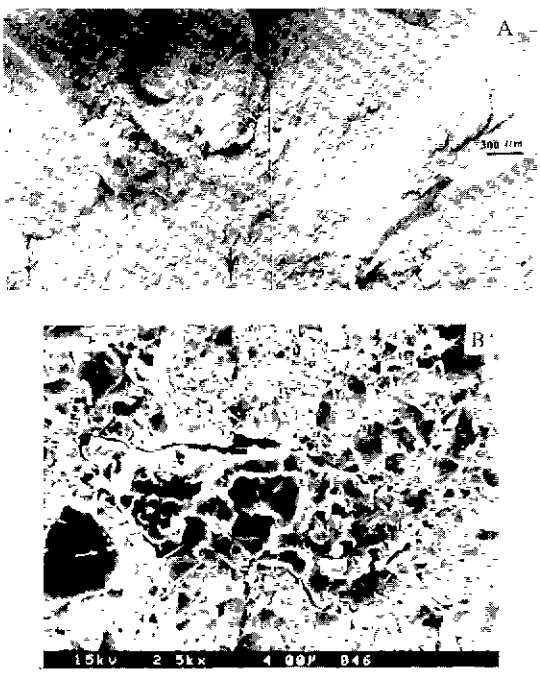

Fig 6. Fracture surface[A] and failure source[B] showing a non-uniformly dispersed cobalt phase[WC-16 Co].

Single pores and/or pore clusters often have been found to be the failure-initiating source in many materials. Several studies[30-32] show that the size of pore is typically in the range of 10 to 200 μm, depending on materials. The strength of the materials generally decrease with increasing pore size and its population. In this study, most WC-Co flexure bars failed due to pores(Fig.7-A & 7-B) which most likely resulted from the cooling stage of sintering. It is known that pores in WC-Co composites are pipe-shaped and the shrinkage of metal phase(cobalt) generally results in about 1 or 2 vol% of porosity[33]. Careful examination of failure sources identified the presence of cracks from machining damage(Fig. 7-C & 7-D) resulting from a typical grinding operation or surface finishing. The flaw (Fig. 7-C) which is seen above the machining damage, acts similar to an indentation crack. If a specimen with machining flaws is subjected to a tensile load, failure will ensue when the stress-intensity factor at the tips of these flaws become critical. The stress-intensity at the tips of these cracks will depend on their orientation to the load axis, the crack size, and the stress concentration effects at the bottom of the machining groove. These parameters will greatly influence the initiation of

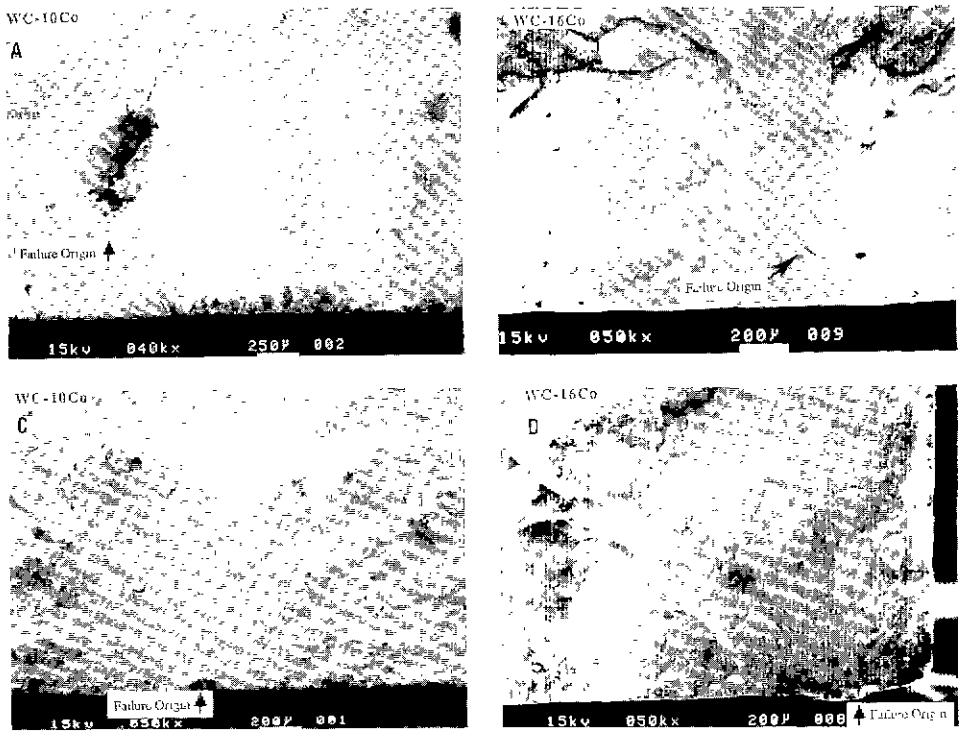

Fig 7. Fracture surface micrographs showing failure origins such as pore[A, B] and machining damage[C, D]

fracture[34,35] Fig.8 shows the microstructure inside a pore in which exaggerated grain growth and no cobalt phase were found. Fig.9 shows another failure mode observed in WC-Co in which crack propagation is continued by connection of small pores. (Lines indicate the boundaries of pores).

SUMMARY

Toughness measurement techniques based on the Palmqvist crack analysis need to be reexamined due to the disagreement of fracture toughness values obtained by different indentation methods. The indentation techniques of Lawn, Marshall and co

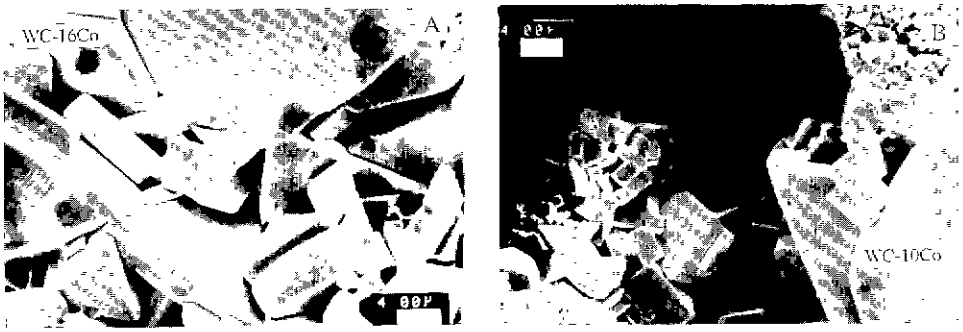

Fig 8. SEM photos showing the interior microstructure of a pore. Pores are major failure-initiating sources in WC-Co composites. Notice that the exaggerated grain growth[A] and the grain boundary without a cobalt phase[B] are quite apparent inside the pore.

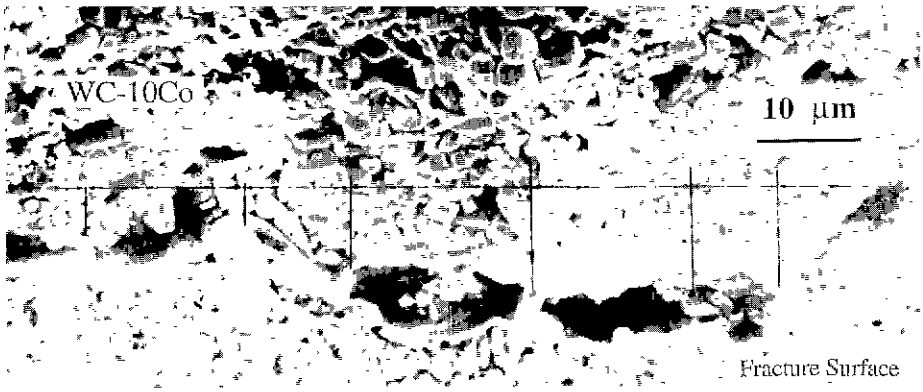

Fig 9. SEM photo shows that fracture occurs by connection of small pores.

-workers[18,19] agree with the large crack techniques for these WC-Co composites. This paper suggests that fracture toughness evaluation by $W=P/4c$ where c is half the surface trace of an indentation crack measured from the center, rather than $W=(P-P_0)/4a$, seems to be acceptable for higher indentation loads. However, more tests are needed to determine the difference in fracture behavior between the radial crack system and the Palmqvist crack system.

Fracture surfaces similar to those seen in glasses and ceramics are observed in WC-Co. The principles of fracture surface analysis that have been developed for other ceramics can be applied to WC-Co composites. Some cobalt bonded WC alloys fail due to machining damage, pores and excessive cobalt binder phase concentration.

REFERENCES

1. F. Osterstock-Thesis, d'Etat, University of Caen, France (1980).
2. H.G. Tattersall and G. Tappin, "The Work of Fracture and its Measurement in Metals, Ceramics and other Materials", *J. Mater. Sci.* **1**, 296-301 (1966).
3. R.W. Davidge and G. Tappin, *Proc. British. Ceram. Soc.*, **15**, 47 (1970).
4. J.L. Chermant and F. Osterstock, "Fracture Toughness and Fracture of WC-Co Composites", *J. Mater. Sci.*, **11**, 1939-1951 (1976).
5. J.L. Chermant, A. Deschanvres, and A. Iost, "Fracture Toughness, Statistical Analysis, and Fractography of Carbides and Metal Composites", in Bradt, Hasselman, Lange (ed.), Fracture Mechanics of Ceramics, Vol. 1, Plenum Press, New York (1974).
6. P. Kenny, "The Application of Fracture Mechanics to Cemented Tungsten Carbide", *Powder Metallurgy*, **14**(27), 22-37 (1971).
7. D.K. Shetty, I.G. Wright, P.N. Mincer, and A. H. Clauer, "Indentation Fracture of WC-Co Cermets", *J. Mater. Sci. Letter* **20**, 1873-1882 (1985).
8. J. Lankford, "Indentation Microstructure in the Palmqvist Crack Regime · Implications for Fracture Toughness Evaluation by the Indentation Method", *J. Mater. Sci. Letter* **1**, 493-495 (1982).
9. J.R. Pickens and J. Gurland, "The Fracture Toughness of WC-Co Alloys Measured on Single -Edge Notched Beam Specimens Precracked by Electron Discharge Machining", *J. Mater. Sci. and Eng.*, **33**, 135-142 (1978).
10. J. Hong and P. Schwarzkopf, "A Comparison Study of Fracture Toughness Measurement for Tungsten Carbide-Cobalt Hardmetals", Chevron Notched Specimen · ASTM STP **855**, 297-308 (1984).

11. R.C. Leuth, "A Study of the Strength of Tungsten Carbide-Cobalt Alloys from a Fracture Mechanics Viewpoint", Ph.D. Thesis, Michigan State University (1972).
12. S.S. Yen, "Fracture Toughness of Cemented Carbides", Master Thesis, Lehigh University (1971).
13. R.C. Leuth, "Determination of Fracture Toughness Parameters for WC-Co Alloys", *Fracture Mechanics of Ceramics Vol.* **2**, 791-806 (1974).
14. E.A. Almond and B. Roebuck, "Precracking of Fracture Toughness Specimens by Wedge Indentation", Metals Technology, **3**, 92-99 (1978).
15. Y.W. Mai, "Thermal Shock Resistance and Fracture Strength Behavior of Two Tool Carbides", *J. Am. Ceram. Soc* **5**, (11-12) 491-494 (1976).
16. C.T. Peter, "The Relationship between Palmqvist Indentation Touthness and Bulk Fracture Toughness for Some WC-Co Cemented Carbides", *J. Mater. Sci.* **14**, 1619-1623 (1979).
17. P. Kenny, "The Application of Fracture Mechanics to Cemented Tungsten Carbides", *Powder Metallurgy* **14**(27). 22-37 (1971).
18. G.R. Anstis, P. Chantikul, B.R. Lawn, and D. B. Marshall, "A Critical Evaluation of Indentation Techniques for Measuring Fracture Toughness : I, Direct Crack Measurements", *J. Am. Ceram. Soc.* **64**(9), 533-538 (1981).
19. P. Chantikul, G.R. Anstis, B.R. Lawn, and D. B. Marshall, "A Critical Evaluation of Indentation Techniques for Measuring Fracture Toughness : II, Strength Method", *J. Am. Ceram. Soc.* **64** (9), 539-543 (1981).
20. J.M. Ogilvy, C.M. Perrott, and J W. Siuter, "On the Indentation Fracture of Cemented Carbide : I -Survey of Operative Fracture", *Wear* **43**(2), 239-252 (1977).
21. C.M. Perrott, "Elastic-Plastic Indentation : Hardness and Fracture", *Wear* **45**(3), 293-309 (1977).
22. R.W. Rice, "Ceramic Fracture Features, Observations, Mechanism, and Uses", Fractography of Ceramic and Metal Failures, ASTM STP 829, J.J. Mecholsky, Jr. and S.R. Powell, Jr. (ed.) 5-103 (1984).
23. J.J. Mecholsky and S.W. Freiman, "Fractographic Analysis of Delayed Failure in Ceramics", ASTM Spec. Tech. Publ., L.N. Gilbertson and R.D. Zipp (ed.) ASTM, Philadelphia, PA, No. **733**, 246-258 (1981).
24. J.J. Mecholsky and S.W. Freiman, "Determination of Fracture Mechanics Parameters Through Fractographic Analysis of Ceramics", ASTM STP 678, ASTM, Philadelphia, PA, 135-150 (1980)
25. J.J. Mecholsky, R.W. Rice, and S.W. Freiman, "Prediction of Fracture Energy and Flaw Size in Glasses from Measurements of Mirror Size", *J. Am. Ceram. Soc.* **57**(10), 440-443 (1974).
26. F.F. Lange, "Processing-Related Fracture Origins : 1. Observations in Sintered and Isostatically Hot-Pressed Al_2O_3/ZrO_2 Composites", *J. Am. Ceram. Soc.*, **66**(6), 396-398 (1983).
27. R.W. Rice, "Sources of Mechanical Failure in Ceramics", p 303-319 in Processing of Crystalline Ceramics, Edited by H.H. Palmour, R.F. Davis, and T.M. Hare, Plenum Press, New York, (1978).
28. J Heinrich and D. Munz, "Strength of Reaction -Bonded Silicon Nitride with Artificial Pores", *Am. Ceram. Soc. Bull.*, **59**(12), 1221-1222 (1980).
29. J.P. Singh, "Effect of Flaws on the Fracture Behaviour of Structural Ceramics : A Review", *Advanced Ceramic Materials* **3**(1), 18-27 (1988).
30. A.G. Evans and R.W. Davidge, "The Strength and Oxidation of Reaction-Sintered Silicon Nitride", *J. Mater. Sci.*, **5**, 314-325 (1970)
31. A.G. Evans and R.W. Davidge, "The Strength

and Fracture of Stoichiometric Polycrystalline UO_2", *J. Nucl. Mater.*, **33**, 249-260 (1969).

32. A.G. Evans and G. Tappin, "Effects of Microstructure on the Stress to Propagate Inherent Flaws", *Proc. Br. Ceram. Soc.*, **20**, 275-297 (1972).
33. R.J. Nelson and D.R. Milner, "Densification Processes in the Tungsten Carbide-Cobalt System", *Powder Metallurgy*, **15**(30), 346-363 (1972).
34. D.C. Cramer, R.E. Tressler, and R.C. Bradt, "Surface Finish Effects and the Strength-Grain Size Relation in SiC", *J Am. Ceram. Soc.*, **60**(5-6), 230-232 (1977).
35. R.E. Tressler, R.A. Langesiepen, and R.C. Bradt, "Surface-Finish Effects on Strength vs Grain Size Relations Polycrystalline Al_2O_3", *ibid.*, **57**(5), 226-227 (1974).